Electrostatic Gating of Ultrathin Films

A.M. Goldman

School of Physics and Astronomy, University of Minnesota, Minneapolis, Minnesota 55455; email: goldman@physics.umn.edu

Annu. Rev. Mater. Res. 2014. 44:45–63

The *Annual Review of Materials Research* is online at matsci.annualreviews.org

This article's doi: 10.1146/annurev-matsci-070813-113407

Keywords

field effect transistors, superconductors, oxides, electric double-layer transistors, metal-insulator transitions, ionic liquids

Abstract

Electrostatic gating of ultrathin films can be used to modify electronic and magnetic properties of materials by effecting controlled alterations of carrier concentration while, in principle, not changing the level of disorder. As such, electrostatic gating can facilitate the development of novel devices and can serve as a means of exploring the fundamental properties of materials in a manner far simpler than is possible with the conventional approach of chemical doping. The entire phase diagram of a compound can be traversed by changing the gate voltage. In this review, we survey results involving conventional field effect devices as well as more recent progress, which has involved structures that rely on electrochemical configurations such as electric double-layer transistors. We emphasize progress involving thin films of oxide materials such as high-temperature superconductors, magnetic oxides, and oxides that undergo metal-insulator transitions.

1. INTRODUCTION

Field effect transistors (FETs) are central to modern information technology, which is critical to the functioning of contemporary civilization. The application of FET principles to ultrathin oxide films can lead not only to changes in resistance, but also to the alteration of the electronic and magnetic properties of these materials (1). The usual approach to changing properties of oxides is to alter their chemical composition, a process that is termed chemical doping (2, 3). The drawbacks of this approach are obvious: Chemical doping is not easily tuned, as a new sample must be produced for each level of doping. In addition to changing the chemical composition, the process may alter the level of disorder, which can also affect the properties. For thin-film systems, electrostatic gating, which is an interfacial phenomenon, can be an attractive alternative to chemical doping, as it can lead to controlled and reversible changes of carrier concentration without, in principle, altering the level of disorder. It has recently become possible to electrostatically gate over a very wide range of carrier concentrations so as to achieve substantial modifications of electronic and magnetic properties. This approach has involved the use of conventional FET configurations employing high-dielectric-constant gate insulators (1) and, more recently, configurations using ion gels or ionic liquids in electric double-layer transistor (EDLT) arrangements (4).

Electrostatic gating is an interfacial phenomenon in that electrostatic screening lengths can be on the order of a lattice constant, resulting in the induced charge being confined to within a few unit cells of the interface. This is a consequence of the relatively high carrier densities found in many materials. For high-transition-temperature (T_c) superconductors and manganites, for which lattice constants are on the order of 4 Å, a single electron per unit cell corresponds to an areal charge density of 6×10^{14} cm^{-2} (1). To fully traverse the phase diagram of such systems, it would be necessary to change carrier concentrations by an amount of this order. To observe phase transitions, materials can be chemically tuned to be near a critical point such that an order-of-magnitude-smaller charge transfer needs to be applied to the surface region. This charge transfer has been accomplished by using FET configurations employing high-dielectric-constant gate insulators (5) and by using the surface charge of a ferroelectric coating the surface of an oxide (6). Tuning chemically to a position on the phase diagram near a critical point is now unnecessary, as by using EDLTs charge transfers in excess of 10^{15} cm^{-2} can routinely be achieved (6). The concept of an electric double layer (EDL), which is explained below, was first put forth in the nineteenth century (7).

This review first considers various device configurations. It then discusses results associated with various oxide systems, focusing on materials that are superconducting and magnetic and on materials that exhibit metal-insulator transitions. A final section summarizes open questions and unresolved issues.

2. DEVICE CONFIGURATIONS

Three configurations have been employed in the electrostatic gating of oxides: (*a*) films in contact with ferroelectric layers, which might be termed ferroelectric FETs; (*b*) conventional FET-like structures using insulating gate dielectrics; and (*c*) EDLTs. In many instances, the induced charge initially populates localized states, and no change in the channel conductance or other properties is obtained until a threshold voltage $\mathbf{V}_T$ is reached. The value of this threshold depends upon factors such as the density of localized states in the oxide, traps at the dielectric-oxide interface, and immobile charges or defects in the dielectric.

2.1. Ferroelectric Field Effect Transistors

This approach to gating involves overcoating a film of interest with a ferroelectric layer and using the polarization field of the ferroelectric to tune the properties of the overcoated film (6, 8–10).

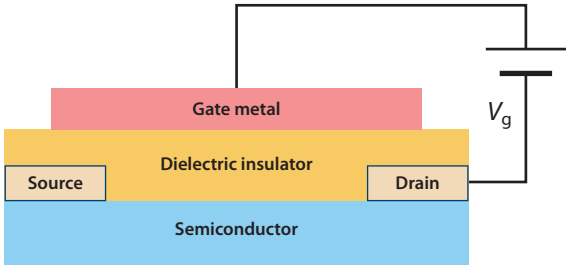

Figure 1

Schematic diagram of a field effect transistor.

The ferroelectric that has been frequently employed is $Pb(Zr_xTi_{1-x})O_3$ (PZT). A sandwich of the film of interest, PZT, and a poling electrode on top of the PZT electrode constitutes the structure. This configuration has been used to modulate the superconducting properties of ultrathin cuprate films and of manganite films. The technique is reversible and leads to a nonvolatile change in state of the film of interest. The latter must be an ultrathin film with systems of interest, as a charge density of order 10^{21} cm^{-3} will lead to a Thomas-Fermi screening length of only a few angstroms (11). The ferroelectric material must be compatible in the process of growth with the material to be controlled. The interface between the two materials must be abrupt and clean. Controlling the structural orientation of both materials of the heterostructure must also be possible.

Although we have referred to these structures as ferroelectric FETs, they are actually a subset of a larger class of multiferroic heterostructures, which simultaneously exhibit ferroelectric and magnetic ordering. These structures, which have the promise of new device applications, have been the subject of considerable activity (12). A discussion of the accomplishments and scientific challenges in this large field is beyond the scope of this review.

2.2. Field Effect Transistors with High-Dielectric-Constant Gate Insulators

In a standard MOSFET (metal oxide semiconductor field effect transistor) device, the gate-induced carrier density is 10^{11}–10^{12} cm^{-2} in the inversion or accumulation layer. Such devices usually employ SiO_2 as the gate insulator. **Figure 1** shows a schematic diagram of a conventional FET. In a typical oxide or correlated electron system, such as a high-temperature superconductor, to add 0.1 charge carriers per unit cell in one monolayer of material, which corresponds to a volume charge density of 5.8×10^{20} cm^{-3}, an areal charge density of 6.7×10^{13} cm^{-2} is needed (1). Thus, the ideal gate dielectric should have a large dielectric constant, high breakdown fields, and lastly a well-defined interface with the material of interest so as to minimize traps and the scattering at defects.

In FETs involving oxide materials, $SrTiO_3$ (strontium titanate, hereafter STO) in both thin-film (13) and single-crystal (14) forms has been used as the dielectric because of its high dielectric constant at low temperatures and good lattice match to many oxides, although the dielectric constant ε for thin films is usually smaller ($\varepsilon \sim 800$ for $T \sim 35$ K) (15) than for single crystals ($\varepsilon \sim 20{,}000$ for $T < 20$ K) at low electric fields (16). Small voltages applied across a film several thousands of angstroms thick can produce very high electric fields. In dielectric crystals, the high voltages needed for these very same fields can lead to breakdown via avalanche processes. However, in films grown by pulsed laser deposition or sputtering, the termination layer cannot be controlled, and surface roughness can be sufficient to prevent the growth of connected ultrathin (<50-Å) films on top. This would not be the case for films grown by molecular beam epitaxy (MBE) (17). Single-crystal gate dielectrics can provide atomically flat surfaces with uniform TiO_2

terminations after surface treatment (18). To reduce the voltages needed to achieve the high electric fields required for significant charge transfers with crystalline gate insulators, commercial substrates can be thinned (19). In configuring FETs employing single crystals, the oxide layer is grown on the TiO_2-terminated face and the gate electrode on the back face.

The semiconductor device industry has been exploring the use of insulators with higher dielectric constants than the dielectric constant of SiO_2 to make ever-smaller devices (20). The dielectric constant of HfO_2, one of the materials used, is 25, whereas the dielectric constant of SiO_2 is only 3.9. If large charge transfers are not essential, or if a dual-gate device is required for fine-tuning, HfO_2 or a similar material can be employed as a gate dielectric.

In the end, the advantage of using crystalline or thin-film STO as a gate insulator with oxide films is that the interfaces between these constituents can be formed without exposure of the dielectric interface layer, which contains polarization charge, to air. This approach eliminates the accumulation of impurities between the two layers. Many oxides grow epitaxially on STO, and there is reasonable compatibility of STO film growth and oxide film growth. However, these compatibilities are not perfect in that there are significant lattice mismatches, and in the case of thin-film heterostructures, the optimum growth conditions for the two layers may be different. Also, the conditions leading to the best interface may be different from the optimal conditions for either layer. As a result, the order at the interface is very dependent on processing conditions, and ideal behavior may not be achievable. An example is the dead layer several unit cells in thickness that is found when $YBa_2Cu_3O_{7-x}$ (YBCO) films are grown on STO (21).

2.3. Electric Double-Layer Transistors

EDLTs are devices that consist of a gate electrode, a semiconductor, a metal, or an insulator into which charge can be accumulated or depleted; source and drain electrodes; and, for purposes of characterization, electrodes for measuring longitudinal and transverse voltages. In place of a solid gate insulator, an ionic liquid (22–24), a polymer electrolyte (25–28), or an ion gel (29) is employed. The latter two are hybrids in that they are polymer ion combinations. We focus our discussion on ionic liquids.

Ionic liquids are salts that are liquid at room temperature. They are effectively solvent-free electrolytes. When incorporated into an FET and gated, positive ions diffuse toward the negative electrode and negative ions to the positive electrode. EDLs form at the electrodes and behave as capacitors with nanometer separation between the ions and the induced charge. The high electric fields that produce large charge transfers in EDLTs have the advantage of providing tunable electric fields without, in principle, restrictions either on the material in which a conductive channel is induced or on its crystalline orientation.

The earliest discussion of EDLs is due to von Helmholtz (7) in 1853. The nanometer spacing of the charge layers is responsible for the large areal charge transfer. The charge transfer can be changed only when the ions of the ionic liquid are mobile, which is in the liquid state and down to temperatures usually somewhat below that at which solidification begins. **Figure 2** shows a schematic of an EDL. Because the induced charge at the EDL occupies a thickness on the order of only a few unit cells of the material under study, it is important that the material to which charge is being transferred be very thin. If it is not, then although one may be able to alter the charge near the surface, the deeper-lying layers may be unmodified, and in the case of superconductors, the proximity effect will come into play, greatly restricting the extent to which the properties of the film can be modified.

Parenthetically, the use of electrochemical techniques to control the electronic properties of materials is actually not particularly new, as Brattain & Garrett (30) first pioneered such techniques

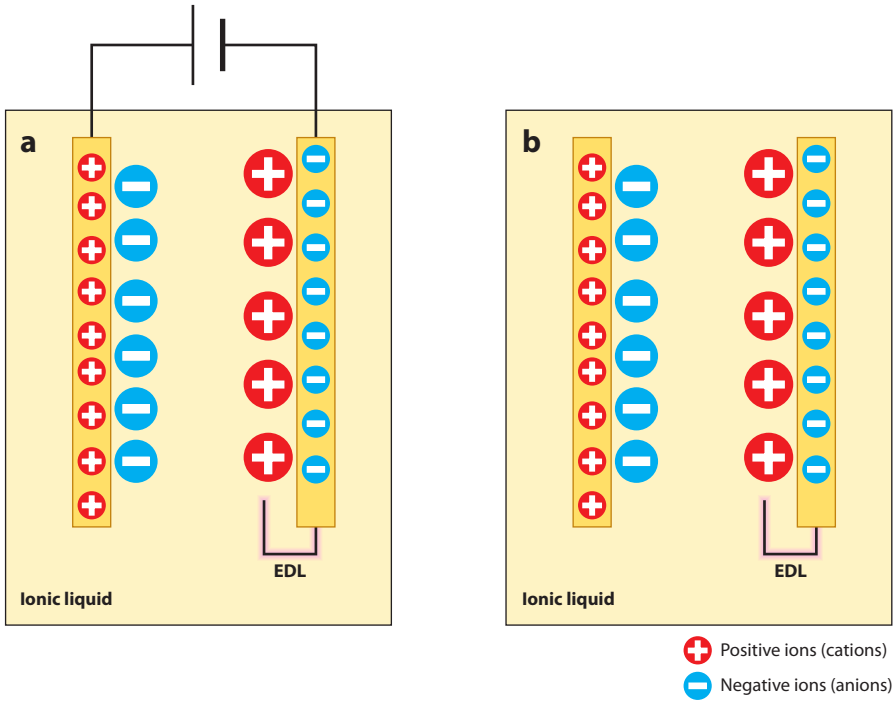

Figure 2

Schematic diagram of the operation of an electric double-layer transistor. (*a*) Upon application of a positive gate bias, anions are attracted to the gate electrode, and cations are repelled, creating an electric double layer (EDL) at the sample surface. (*b*) Ions are frozen in position with the gate bias removed.

in the 1950s. McDevitt and collaborators (31) first used these techniques approximately 20 years ago to control superconductivity.

The advantage of EDLTs is the possibility of charge transfers up to two orders of magnitude larger than achievable by using conventional solid dielectrics. EDLTs have been used to induce or modify superconductivity in ZrNCl (32, 33), STO (34, 35), $KTaO_3$ (36), MoS_2 (37, 38), $La_{2-x}Sr_xCuO_4$ (39, 40), YBCO (21, 41), La_2CuO_4 (42), and InO_x (43). The technique has also been employed in the tuning of the properties of manganites such as $La_{0.8}Ca_{0.2}MnO_3$ (44). In addition, ionic liquids have been used to traverse metal-insulator transitions in a number of systems (45–53).

The possibility of extreme charge transfer using ionic liquids comes with a price. The charge accumulation or depletion layers formed by using EDLTs contain high electric fields and high electric field gradients. Furthermore, work on organic semiconductors has revealed that, with increasing carrier density, there is a maximum in channel conductance associated with a decrease in carrier mobility (54). Thus, electrostatic doping may not be completely equivalent to chemical doping to the same charge level and may actually increase disorder with increased doping.

There is also the question of the temperature ranges over which various properties manifest themselves (23). There is nonzero ionic conductivity when the ionic liquid is in the liquid state. There is a glass transition to a solid phase, which is found at a material-dependent temperature. Ionic mobility may persist to a lower, material-dependent temperature. As a result, there is a

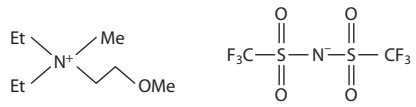

Figure 3

Chemical formula of DEME-TFSI [*N*,*N*-diethyl-*N*-(2-methoxyethyl)-*N*-methylammonium bis(trifluoromethylsulfonyl)imide]. Me and Et refer to methyl and ethyl groups, respectively.

window of temperature over which ions are mobile; this range extends from room temperature down to ~190 K in the case of a commonly used ionic liquid, DEME-TFSI [*N*,*N*-diethyl-*N*-(2-methoxyethyl)-*N*-methylammonium bis(trifluoromethylsulfonyl)imide] (32, 55) (see **Figure 3**). Therefore, in the case of an investigation of a low-temperature phenomenon such as superconductivity, it is necessary to cycle the EDLT in temperature to change the carrier concentration. This is a serious complication for studies below 1 K that involve a complex refrigeration apparatus.

The extent of irreversible chemical degradation at various temperatures and gate voltages is also unknown. For different combinations of ionic liquids and materials of interest, there appear to be temperatures and gate voltages below which chemical effects are minimal. However, information regarding such effects is not well established.

There is also evidence that the response of some materials to electrostatic gating using ionic liquids involves electric field–induced oxygen vacancy formation rather than charge transfer (53). Whether this feature is common to all experiments involving oxides in which the oxygen concentration controls the electronic properties is an open question. This issue is a part of the broader question of the mechanism for the alteration of electronic and magnetic properties of materials by electrostatic gating.

Ionic liquids present problems due to their lack of volatility and liquid nature at room temperature (56). It may be difficult to ensure an impurity-free interface between the ionic liquid and the interface material at a level that is possible for the case of a vapor-deposited gate insulator and an FET device formed in an in situ process.

Whereas the Thomas-Fermi screening length gives the length scale for charge penetration, in the case of conventional FETs, the situation is more extreme for EDLTs, and there is no completely satisfactory model of ion organization in an ionic liquid and of the induced charge in a solid. In the Helmholtz model, an EDL consists of (*a*) a single ionic layer in solution in contact with the solid surface and (*b*) a single layer of charge in the solid (7). The potential difference between the gate and the solid being gated manifests itself only at the EDLs between the gate and the ionic liquid and between the solid and the ionic liquid. The confinement of potential drops to these ultrathin regions leads to high levels of charge accumulation. The layer of charge in the ionic liquid is bounded by what is referred to as the outer Helmholtz plane. The thickness of this layer is essentially independent of the thickness of the electrolyte layer. This configuration is dramatically different from the case of conventional dielectrics, in which the potential drop is a linear function of the distance between the gate and the solid in a parallel-plate configuration. The most commonly used variant of the Helmholtz model is the Gouy-Chapman-Stern model (57). This model extends the Helmholtz picture by allowing for the thermal motion of the counterions, which compensate for the charge of the material surface. The penetration of the charge layer in the solid is on the order of the ion size, which is at most only several atomic layers thick. Thus, the details of the interface are of crucial importance, even when there is less control of its quality relative to interfaces formed by using in situ processes.

3. MATERIAL SYSTEMS

By using variants of the configurations described above, external control of charge density up to significant fractions of an elementary charge per unit cell has been possible. Therefore, ground states of many materials can be dramatically affected by charging, and as a result, striking changes are possible with selected materials. This development has made possible the exploration and characterization of metal-insulator transitions, superconductor-insulator transitions (SITs), and transitions in which magnetic properties are modified. In the following subsections, we discuss major results from each of these three areas. We begin with a discussion of superconductivity.

3.1. Superconductors

Attempts to modify the properties of superconductors began 54 years ago with the work of Glover & Sherrill (58). They observed miniscule changes in the T_cs of 70-Å-thick In and Sn films grown on 5-μm-thick ruby mica substrates provided with back gates. The tiny effect observed was not unexpected, as the number of added electrons was less than 10^{-4} of the total number of atoms in the film. A second metal field effect study of note is the work of Stadler (59), which involved ferroelectric polarization charging. This technique produced a change in the T_c of 0.0013 K of a 160-Å-thick Sn film grown on triglycine sulfate, which served both as a substrate and as the source of ferroelectric polarization. The response was again small because of the high carrier density of a metal, and the thickness of the film was substantially greater than the Thomas-Fermi screening length.

Fiory & Hebard (60) investigated electrostatic gating of composite In/InO_x films that were 5 to 10 nm thick. These films have much lower carrier densities (10^{20} cm^{-2}) relative to those of metal films (10^{22}–10^{23} cm^{-2}). The charge-induced change in the superconducting T_c was estimated to be ∼8%. This shift in T_c was achieved by using a 13-μm-thick Mylar film insulator. A 500-V bias resulted in a charge transfer of 2.2×10^{11} carriers cm^{-2}. The same group performed similar studies with a 100-Å-thick Al_2O_3 dielectric and claimed a charge transfer of 1.25×10^{13} carriers cm^{-2} and substantially greater changes in T_c. For these InO_x films modeled as free-electron gases, static charge penetration was still only ∼2 Å. Thus, the films were not sufficiently thin to result in a substantial modulation of T_c. Also contributing to the weakness of the effects were the low dielectric constants of the gate insulators and their relatively large thicknesses, which greatly reduced their specific capacitances.

Hebard and collaborators (61) were the first to use ionic liquid EDLTs to study amorphous InO_x films. Using both coplanar (side) gates and overlay gates, they demonstrated electric field–induced resistance changes on the order of a factor of 10^4 for 40-Å-thick films. The areal capacitances and field effect mobilities significantly exceeded those achieved by using AlO_x gate insulators. The ionic liquid used for this work was 99.5% pure EMI-BETI [1-ethyl-3-methylimidazolium bis(trifluoromethylsulfonyl)imide]. No systematic attempt was made to optimize the choice of ionic liquid, although careful efforts were made to keep the substrates and liquid containers clean and free of contaminants. The measurements were carried out from liquid nitrogen temperatures to room temperature, so a SIT was not observed.

More recently, Lee et al. (62) carried out a study of the SITs of amorphous InO_x films by using ionic liquid EDLTs. Film thicknesses ranged from 6 to 10 nm. The ionic liquid DEME-TFSI was used as a gate dielectric with a Pt coil top gate. An insulating film was tuned into the superconducting state, and a superconducting film was tuned into the insulating state. The systematic evolution from insulating to superconducting behavior at different gate voltages was documented. An iconic feature of magnetoresistance studies of disordered InO_x films is the appearance of a

giant magnetoresistance peak in the magnetic field–tuned insulating regime. The evolution of this peak with disorder has been studied. Electrostatic gating has permitted the study of the peak's evolution with carrier concentration.

Earlier experiments that yielded more quantitative results regarding the SIT are those of Parendo and collaborators (63). In these studies, superconductivity was induced electrostatically in amorphous Bi insulating films ~1 nm thick in a configuration in which a high-dielectric-constant material (STO) that was mechanically thinned to leave parallel surfaces 50 μm apart was used both as a substrate and as a gate insulator (63). In these experiments, the ground state of the films was changed from insulating to superconducting by tuning charge.

High-temperature superconductors such as those in the cuprate family are the quintessential examples of strongly correlated electron systems (1). They, together with the colossal magnetoresistance manganites, have been the focus of considerable attention because of the plethora of new and interesting behaviors they exhibit. Many of the ideas that are bedrock principles in the understanding of conventional metals and semiconductors fail in this context, suggesting the need for new approaches.

An important feature of correlated electron systems is the competition between distinct electronic phases with respect to changes in chemical composition, strain, or external fields that change the system from one behavior to another (64). This feature has served as the impetus for research on FET configurations, with the idea of employing electrostatic gating with charge density as the tuning parameter so as to foster fundamental understanding.

In general, at low levels of doping, cuprates are antiferromagnetic insulators. At higher levels, they become superconductors; the temperature of the transition to the superconducting state as a function of carrier concentration takes a characteristic dome shape. The normal state of underdoped superconductors is termed the pseudogap regime and has been the subject of considerable interest (3). Crucially, the relevant range of doping is between 0 and 0.2 carriers per unit cell, corresponding to an area density of $0 < n_{2d} < 10^{14}$ cm^{-2}. The other feature of these superconductors is their layered crystal structures with electronic properties concentrated in the CuO_2 planes. **Figure 4** shows a schematic phase diagram of hole-doped cuprates.

A number of electrostatic gating studies have used conventional and ferroelectric FET configurations. Charge was introduced by reversing the polarization of a ferroelectric layer of PZT, as was discussed above (6). Studies of the resistance variation upon this reversal as well as Hall effect studies showed that the changes in the electronic properties were consistent with an alteration in the average carrier density equal to the measured polarization divided by the film thickness.

Mannhart (5) used an FET configuration with a high-dielectric-constant insulator to shift the T_c of an $YBa_2Cu_3O_7$ film by 8 K. The T_c of an $NdBa_2Cu_3O_{7-\delta}$ film was shifted by 3.5 K in a structure in which STO served as both the substrate and the gate insulator (17). The T_c of Ca-doped $SmBa_2Cu_3O_y$, an electron-doped material, was enhanced by the addition of electrons (65). An FET device consisting of an $Nd_{1.2}Ba_{1.8}Cu_3O_x$ film grown on a (100) STO substrate, overlaid with an Al_2O_3 insulator and an Au gate, was used to demonstrate reversible changes of the hole density (66). Superconductivity was also induced in an insulating film of this material that was eight unit cells thick. By gating an underdoped two-unit-cell-thick $La_{2-x}Sr_xCuO_4$ film with an HfO gate insulator with a high dielectric constant, relative changes of the areal superfluid density n_s were observed in measurements of the film kinetic inductance (67). **Figure 5** shows a schematic of the FET configuration used in these experiments.

The relationship between the critical temperature T_c, the mobile areal carrier density in 2D, and the zero-temperature magnetic in-plane penetration depth in very thin underdoped $NdBa_2Cu_3O_{7-\delta}$ films near the SIT was also explored (68). In the three- to

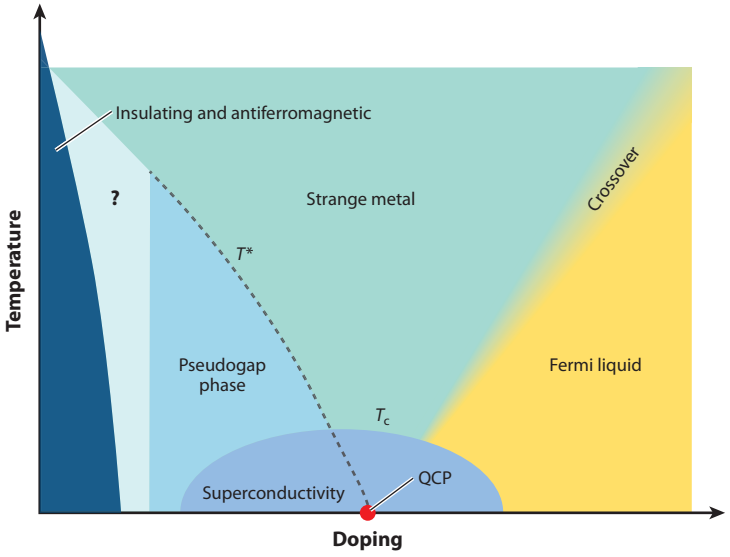

Figure 4

Schematic of the hole-doped cuprate phase diagram. At very low levels of electron-hole doping, cuprates are insulating and antiferromagnetic. At increased doping levels, they become conducting, and the exact temperature and doping level determine which phase they will be in. At temperatures below T_c, they become superconducting, and at temperatures above T_c but below T^*, they are in the pseudogap phase. The boundary of the pseudogap region at low doping levels is unknown. The transition between the Fermi-liquid phase and the strange-metal phase occurs gradually (by crossover). QCP denotes the quantum critical point at which some researchers conjecture that T^* goes to absolute zero. From Reference 3.

four-unit-cell-thick films used in this study, T_c modulations of more than 10 K were achieved, corresponding to induced-charge densities on the order of 0.7×10^{14} cm^{-2}.

X-ray absorption spectroscopy was used to study the doping mechanism of the CuO_2 planes in $Nd_{1+x}Ba_{2-x}Cu_3O_7$ compounds (69, 70). Such study used a back-gated film on a STO substrate. Such field effect experiments in ultrathin films are usually interpreted by supposing that the

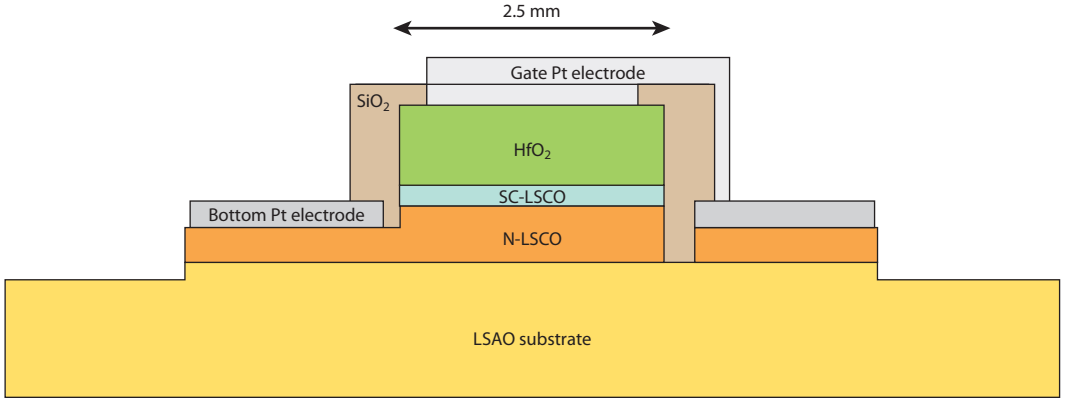

Figure 5

Cross section of a multilayer field effect transistor device. LSAO, lanthanum strontium aluminate substrate; LSCO, $La_{2-x}Sr_xCuO_4$; N-LSCO, normal LSCO; SC-LSCO, superconducting LSCO. Adapted from Reference 67.

induced charges develop into carriers in the CuO_2 conducting planes. Polarization charges in both insulating and superconducting films are confined mainly to the charge reservoir and, in particular, to the CuO chains. The characteristics of the charge reservoir layer determine the doping of the CuO_2 planes, achieved by transfer of a fraction of the total injected holes. Within the wider range of high-temperature superconductors, the compound $Nd_{1+x}Ba_{2-x}Cu_3O_7$ belongs to the 123 family, in which, besides CuO_2 planes, there are CuO chains within a charge reservoir. Transmission electron microscopy studies demonstrated that the first layer at the film/substrate interface belongs to the charge reservoir. As a consequence, these results may be specific to the case of 123 compounds of this structural configuration.

The use of EDLT structures has resulted in a revolutionary change in the possibilities for gating of oxides. Dhoot et al. (71) studied thin films of $YBa_2Cu_3O_{7-\delta}$ and constructed two types of devices, one employing a poly(ethylene oxide)/lithium perchlorate (PEO/$LiClO_4$) electrolyte and the other the ionic liquid EMIM-TFSI [1-ethyl-3-methylimidazolium bis(trifluoromethylsulfonyl)imide]. The samples using the polymer electrolyte were in a top-gated configuration with a planar gate. The configuration using an ionic liquid was not specified. With 10- and 30-nm-thick $YBa_2Cu_3O_7$ films, significant changes in T_c were produced by modest gate voltages, but the SIT was not traversed by depleting carriers. This situation is presumably a consequence of the charge penetration length being much smaller than the film thickness. Dhoot et al. also found that, although the T_c and channel conductance could be changed by the gate voltage, cuprate films were not entirely stable when in contact with the electrolyte.

Dhoot et al. (71) and Chandrasekhar et al. (72) also considered the possibility of an electric field–driven movement of dopant atoms in the conductive channel (oxygen anions). These atoms could also modulate the mobile carrier density, but in a manner unlike that expected in a purely capacitively coupled device. This modulation could proceed by electromigration of mobile ions inside the lattice, followed by subsequent modification of the chemical structure. Control experiments demonstrated the reversibility of the gating effect but could not rule out the possibility of slow, field-induced changes in the atomic structure.

EDLTs have been used to tune the SIT of $La_{2-x}Sr_xCuO_4$ (LSCO) (39, 40); of YBCO (21, 41); and, very recently, of oxygenated and superconducting $La_2CuO_{4+\delta}$ (δ-LCO) (42). In each of these studies, the ionic liquid DEME-TFSI was employed. The work on LSCO involved the synthesis by ozone-assisted MBE of epitaxial films that were one unit cell thick (39, 40). These films were grown on top of a buffer layer of insulating LCO. Many resistance-versus-temperature [$R(T)$] curves at different gate voltages were recorded, and the SIT was traversed with detailed enough data to carry out an accurate finite-size scaling analysis (73). The effective hole concentration was obtained by assuming that Drude conduction described the high-temperature behavior of the films and that, as such, the relative carrier population was proportional to the inverse of the resistance. **Figure 6** shows the result of the study of an underdoped and insulating film. The data collapse into two branches: one for films that are superconducting and a second for insulating films. The success of scaling implies the occurrence of a direct SIT, the details of which are discussed in References 39 and 40. There are reasons to approach such a conclusion with caution. The scaling analysis involves only data down to $T = 4.3$ K, and there are indications of local minima in the $R(T)$ curve at the lowest temperatures. The implication is that the scaling may break down at lower temperatures than those of these measurements.

The results of studies of YBCO films grown by high-pressure oxygen sputtering were somewhat different (21). For thicknesses less than or equal to six unit cells, the films were insulating, whereas thicker films were superconducting. Thus, a seven-unit-cell-thick film may have an active superconducting layer that is only one or two unit cells thick. The EDLT device was top gated. By starting with a superconducting film by depleting holes (adding electrons), the SIT was

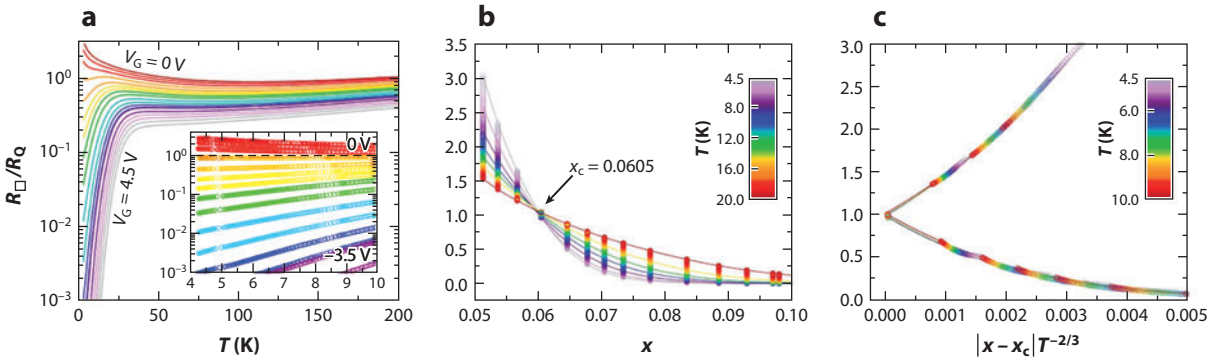

Figure 6

Superconductor-insulator transition of LSCO driven by electrostatic gating. (*a*) Temperature dependence of the sheet resistance normalized to the quantum resistance for pairs, $R_Q = h/4e^2$, of an initially heavily underdoped and insulating film. The device employs a coplanar Au gate and DEME-TFSI ionic liquid. The carrier density, fixed for each curve, is tuned by varying the gate voltage from 0 to 24.5 V in 0.25-V steps; an insulating film becomes superconducting via a quantum phase transition. The inset highlights a separatrix independent of temperatures less than 10 K. The open circles are the actual raw data points; the black dashed line corresponds to $R_Q = 6.45$ kΩ. (*b*) Isotherms of the same data, as a function of doping x, at fixed temperatures less than 20 K. Each vertical array of (~100) data points corresponds to one fixed carrier density, that is, to one curve in panel *a*. The colors refer to the temperature, and the continuous lines are interpolated for selected temperatures (4.5, 6.0, 8.0, 10.0, 12.0, 15.0, and 20.0 K). The crossing point defines the critical carrier concentration $x_c = 0.06 \pm 0.01$ and the critical resistance $R_c = 6.45 \pm 10$ kΩ. (*c*) Scaling of the same data with respect to the quantity $|x - x_c|T^{-1/\nu z}$, with $\nu z = 1.5$. For 4.3 K $< T <$ 10 K, the discrete groups of points of panel *b* collapse accurately onto a two-valued function, with one branch corresponding to x larger than and the other to x smaller than x_c. The critical exponents are identical on both sides of the superconductor-insulator transition. The raw data points cover the interpolation lines almost completely, but not close to the origin. Adapted from Reference 39.

traversed. By using the same approach to inferring the carrier concentrations as was employed in the study of LSCO (39), a phase diagram was constructed and is plotted in false colors as shown in **Figure 7**. The resemblance to the bulk phase diagram is striking. A scaling analysis similar to that performed on LSCO films was carried out and worked down to a temperature of ~6 K. The breakdown of scaling is a consequence of the nonmonotonic behavior of $R(T)$ at low temperatures for gate voltages close to criticality. These results suggest that the SIT is not direct and may involve intermediate phases and multiple quantum critical points.

Accumulation of holes by gating with negative rather than positive voltages was also possible (41). This accumulation of holes resulted in the tuning of T_c across the top of the superconducting dome. This behavior cannot be achieved by manipulating solely the oxygen concentration of YBCO. Starting from an underdoped film, the T_c increased and the normal-state resistance decreased with increasing hole concentration. However, at a hole concentration greater than that at optimal doping, the T_c decreased with increasing hole concentration, but the normal resistance increased. The former behavior is the same as, but the latter behavior is the opposite of, that found for all chemically doped cuprates.

The Hall effect along with the longitudinal resistance of the films was studied. The Hall number $n_H = 1/R_H e$, where R_H is the Hall coefficient determined from the slope of the linear fit of the Hall resistance versus magnetic field, exhibited a peak at a carrier concentration just short of that corresponding to optimal doping. Similar behaviors have been found in bulk systems, although at higher fields and lower temperatures. Such behaviors have been commonly interpreted as evidence of a change in the electronic structure of the conductive channel.

The electron-doped regime of compounds such as YBCO cannot be reached by oxygen manipulation because of the limits of chemical stoichiometry. This regime can be achieved by doping La

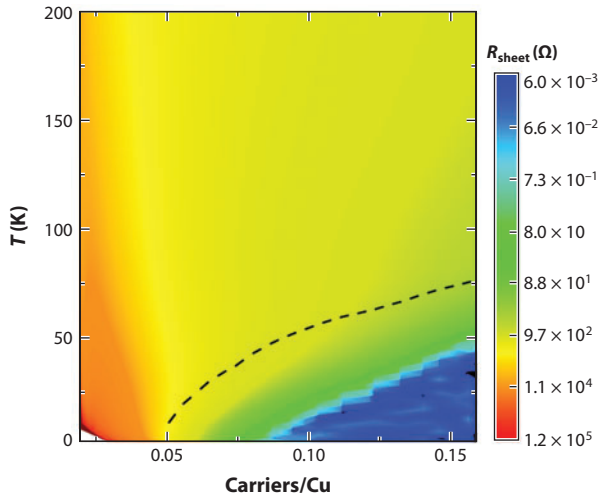

Figure 7

Color plot of the resistance versus temperature at various carrier concentrations. This plot can be interpreted as a phase diagram. Different colors represent different sheet resistances. The dashed line is the temperature at the onset of the superconducting transition. The white area in the bottom left-hand corner is a regime with nonlinear *I-V* curves. From Reference 21.

on both the Y and Ba sites. Nojima et al. (74) demonstrated extreme hole reduction and subsequent electron accumulation in YBCO films by using an electrochemical technique. However, there was no sign of superconductivity. They found that an *n*-type regime with some signature of superconductivity could be achieved by using an EDLT configuration that employed DEME-TFSI as the gate insulator. Reversibility of the charging process in these particular studies was never confirmed, so the observed behavior may have been a consequence of electrochemistry rather than one of electrostatics (75).

The SIT of four-unit-cell-thick films of MBE-grown and oxygen-doped δ-LCO has also been studied (42). A top-gated EDLT was used to transfer charge to the film. Charge transfers were determined by integrating the transient current that flowed in response to changes in gate voltage. The most striking result was the finding of an in-plane, low-temperature anisotropy of the electronic properties of the films. This anisotropy is at a minimum at the SIT and occurs at the same hole concentration as a maximum in the Hall resistance found at high temperatures. This finding suggests that the SIT of electrostatically doped δ-LCO films is electronically driven.

3.2. Oxide Ferromagnets

The most interesting examples of work on magnetic materials are changes effected in the case of colossal magnetoresistance manganites. These compounds have properties that vary as the carrier concentration is changed; such compounds have a range of ferromagnetic metallic, charge-ordered antiferromagnetic insulating, and nonordered phases (2, 76). Some of these properties are coexistent, depending upon the particular material. The very first studies involved FET configurations using pulsed laser–deposited (PLD) films of $Nd_{0.7}Sr_{0.3}MnO_3$ with a PLD STO film as a gate dielectric (77). Early quantitative studies involved the use of the polarization field of PZT to electrostatically modulate the metallicity of a variety of manganites and especially ultrathin manganite $La_{1-x}Sr_xMnO_x$ (LSMO) films doped to be near the metal-insulator transition

(8). Such studies were followed by experiments in which the ferromagnetic Curie temperature was reversibly shifted by 35% (78). The electronic origin of these behaviors was later demonstrated by X-ray absorption spectroscopy (9).

Ultrathin films of $La_{0.8}Ca_{0.2}MnO_3$ (LCMO) with a composition close to that of the metal-insulator transition were grown on single-crystal STO substrates that were thinned mechanically and coated on the back surface with a gate electrode. The response to a gate electric field was ambipolar (79). The decrease in resistance found at low temperatures in this work was attributed to the development of a pseudogap in the density of states. Furthermore, the magnetic coercivity could be altered electrostatically, although not reversibly. [Chiba et al. (80) first demonstrated reversible tuning of magnetic coercivity by using the dilute magnetic semiconducting system (In, Mn)As.]

More substantial modulation of the ferromagnetic Curie temperature on the order of 43 K was reported by using PLD-grown LSMO films with STO as a dielectric and in a novel side-gate configuration (9). The resistivity modulation was up to 250% at low temperatures. Films that exhibited this behavior were seven unit cells thick. Thinner films were insulating and were almost insensitive to field effect gating. In effect, the first six unit cells of material appeared to be dead. In terms of charge per unit area, this configuration attained 1.6×10^{12} cm^{-2} at 300 K and 1.1×10^{13} cm^{-2} at 10 K.

Dhoot et al. (44) exceeded this level of charge transfer by employing an EDLT configuration with the ionic liquid EMIM-TFSI and the polymer electrolyte PEO/$LiClO_4$ to electrostatically gate LCMO. For positive gate bias, electron doping drove a transition from ferromagnetic metal to an insulator. Dhoot et al. claimed that the charge-doped layer extended 5 nm into the film thickness, corresponding to an areal carrier density of 2×10^{15} cm^{-2}. This depth of penetration is greater than any estimate based on either ion size or the Thomas-Fermi screening length and relies on consideration of the effects that an undoped shunt layer away from the active surface might have on the response to gating. This conclusion must be viewed with care, as it does not take into account the possibility that the layer of the film contiguous with the substrate may be dead.

3.3. Systems Exhibiting Metal-Insulator Transitions

In this section, we focus on work on metal-insulator transitions in oxide ultrathin films. We omit a discussion of work on thin single-crystal samples. For the interested reader, a recent review of EDLTs has broader coverage (24). The other topic that is not discussed here involves work on ultrathin films of metals not involving superconductivity (81).

The main focus here is on nonferromagnetic correlated electron materials, in which electrostatic gating might be used to produce a device conceptually different from the usual FET of Si technology. Attention has been directed toward the rare earth nickelate family of compounds and to VO_2, which is a Mott insulator. We first consider the rare earth nickelates, which are a family of perovskites that exhibit well-defined metal-insulator transitions as a function of temperature. The one exception to this is $LaNiO_3$ (LNO), which remains metallic in bulk down to the lowest temperatures. Its epitaxial compatibility with numerous materials makes it a choice electrode material for various oxide devices. A metal-insulator transition can occur in LNO by introducing oxygen vacancies. Epitaxial films grown on (001) STO exhibit a metal-insulator transition if their thicknesses are reduced to fewer than eight unit cells. Electric fields have been used to tune the metal-insulator transition of ultrathin films of LNO. By using an FET configuration in which the STO substrate serves as a gate dielectric, the temperature of the transition is tunable by up to 24 K, and overall resistivity changes of 10% are achieved (82). These films exhibit *p*-type conduction, as established by Hall effect measurements.

Two different groups (83, 84) have also demonstrated electrostatic control of the metal-insulator transition of epitaxial films of $NdNiO_3$ (NNO) by using EDLT configurations

employing ionic liquids. NNO exhibits a sharp temperature-driven, first-order metal-insulator transition, whose mechanism is still under discussion. A representative result from these studies is a shift of 40 K in the temperature of the metal-insulator transition, with the resistivity just above the transition shifted by one order of magnitude. The thickness dependence of the effect raises the issue of whether effects other than electrostatic gating are responsible for the observations.

VO_2 FETs, the subject of intensive research driven by technology, may provide an alternative to Si FET technology. This compound exhibits a thermally induced transition at 340 K, and its dynamics would appear to make it suitable for switching device use (85). The mechanism for the transition is not understood, and there would be a need to separate the electronic transition from the structural phase transition. The latter is a transition from a high-temperature rutile structure to a low-temperature monoclinic structure. Temperature, pressure, and chemical doping can affect the phase transition.

Electrostatic modulation of the transition in VO_2, although studied by many, has certain difficulties (50, 52, 53, 86–90). The relatively high carrier density determined from the Hall effect restricts electrostatic gating to a very thin channel, which mandates ultrathin films. Moreover, conventional oxide gate insulators such as SiO_2, Al_2O_3, and HfO_2 require high gate voltages, which result in substantial leakage currents. Ionic liquid–based EDLTs provide an alternative approach, which several groups have used, and raise some important issues regarding the use of EDLTs.

DEME-TFSI was recently used to induce a metal-insulator transition in PLD-grown epitaxial VO_2 films by using an EDLT configuration (52) (**Figure 8**). These results were ascribed to the introduction of only a small number of carriers. In essence, the conventional picture was asserted to not apply in that electrostatic charging at the interface purportedly drove the previously localized carriers in the bulk of the film, leading to a 3D metallic ground state. This scenario would be consistent with the destabilization of the Mott insulating state of VO_2 that depends critically on half-filling of an electron band. Preliminary X-ray structure data support this electrostatically gated metal-insulator transition being accompanied by a structural transition from a metallic tetragonal (rutile) phase to an insulating monoclinic phase.

This interpretation has been challenged by very recent work that demonstrated that electrolytic gating leads not to electrostatically induced carriers but to the electric field–induced creation of oxygen vacancies with oxygen migrating from the oxide film into the ionic liquid (53). These measurements were performed by using PLD epitaxial films grown on both TiO_2 and Al_2O_3 substrates. The films on the former substrates were 10 nm thick, whereas those on the latter substrates were 20 nm thick. An approximately 100-nL droplet of the ionic liquid HMIM-TFSI [1-hexyl-3-methylimidazolium bis(trifluoromethylsulfonyl)imide] covered the channel and lateral gate electrode. The process of gating was hysteretic but reversible. After switching to the high-conductance state, the devices were stable with zero gate voltage for many days, even when the ionic liquid was removed by using isopropyl alcohol. X-ray photoelectron spectroscopy (XPS) was used to demonstrate the complete removal of the ionic liquid. Films grown on both substrates showed the same behavior. The insulating phase could be recovered either by reverse gate voltages or by annealing in oxygen at ~200°C. Furthermore, XPS studies of the oxidation state of V suggested the formation of oxygen vacancies, which were stable in the absence of the EDL. ^{18}O was incorporated within the VO_2 channels during reverse gating. The presence of oxygen in the chamber suppressed the source-drain current when the structure was gated into the metallic state. These results suggest that, even though the energy required to create an oxygen vacancy in VO_2 in the absence of an electric field is high, electric field–induced migration of oxygen into and out of the ionic liquid may be an alternative explanation for the response of VO_2 to gating involving EDLT configurations. This mechanism may be at work in the behavior of the other systems discussed above.

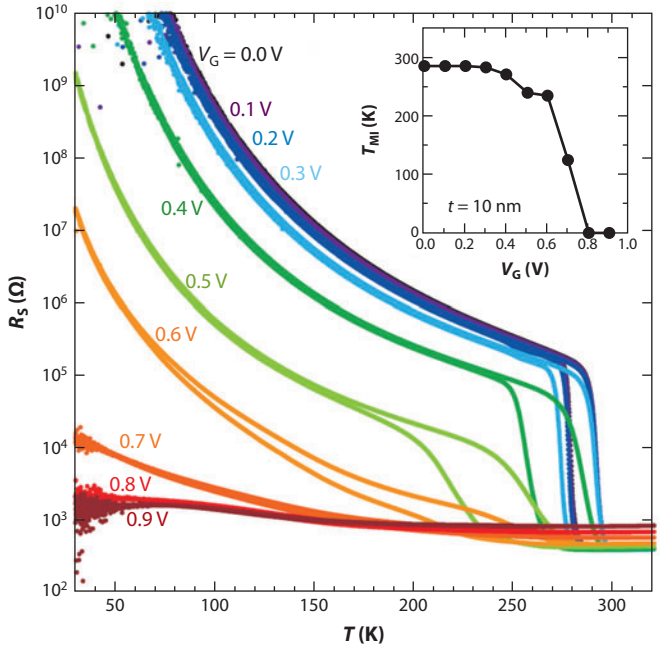

Figure 8

Effect of electric field on the transport properties of a 10-nm-thick, strained VO_2 film. This is a plot of the temperature dependence of the sheet resistance (R_S) for such a strained VO_2 film with different gate voltages (V_G). The inset shows the resulting phase diagram. The transition temperature (T_{MI}) is defined as the average of the two inflection points (for cooling and warming, respectively) in plots of d[ln(R_S)]/d(1/T) versus temperature. Adapted from Reference 52.

4. SUMMARY

This review presents a variety of examples of electrostatic gating of oxides. To a certain extent, results can be anticipated by employing what is known regarding the materials from studies of the bulk. However, a plethora of additional issues are relevant. Electrostatic gating is largely a surface effect, and the surface properties of complex oxides are not fully understood. In contrast to the case for semiconductor FETs, the injected charge may be concentrated within a few unit cells of the surface rather than spread out over hundreds of angstroms. In the EDLT configuration, there are extraordinarily large electric fields. How these fields affect the behavior of defects and how they may influence the positioning of ions are largely unknown. The physics of oxides under these conditions may be different from that of the same materials in bulk. In the case of EDLT configurations, which have yielded spectacular results, it is not clear that reversible electrical behavior precludes the action of electrochemical processes that are also reversible. In the context of oxide electronics, the most effective approaches to altering the properties of oxides in terms of charge transfer values may not yield useful devices because of slow time constants and constraints on temperatures at which the gate bias must be changed.

DISCLOSURE STATEMENT

The author is not aware of any affiliations, memberships, funding, or financial holdings that might be perceived as affecting the objectivity of this review.

ACKNOWLEDGMENTS

The author thanks Xiang Leng, Yeonbae Lee, Javier Garcia-Barriocanal, Joseph Kinney, J.J. Nelson, Stephen Snyder, Terry Bretz-Sullivan, and Boyi Yang for very helpful discussions regarding electrostatic gating. He also thanks Dan Frisbie and Yoshihiro Iwasa for introducing him to the EDLT. This work was supported in part by the Division of Materials Research of the National Science Foundation under grants DMR-1209578 and -1263316 and by the US-Israel Binational Science Foundation under grant 2008299.

LITERATURE CITED

1. Ahn CH, Bhattacharya A, Di Ventra M, Eckstein JN, Frisbie CD, et al. 2006. Electrostatic modification of novel materials. *Rev. Mod. Phys.* 78:1185–212
2. Imada M, Fujiimori A, Tokura Y. 1998. Metal-insulator transitions. *Rev. Mod. Phys.* 70:1039–263
3. Varma C. 2010. High-temperature superconductivity: Mind the pseudogap. *Nature* 468:184–85
4. Yuan H, Shimotani H, Tsukazaki A, Ohtomo A, Kawasaki M, Iwasa Y. 2009. High-density carrier accumulation in ZnO field-effect transistors gated by electric double layers of ionic liquids. *Adv. Funct. Mater.* 19:1046–53
5. Mannhart J. 1996. High-T_c transistors. *Supercond. Sci. Technol.* 9: 49–67
6. Ahn CH, Gariglio S, Paruch P, Tybell T, Agtognazza L, Triscone J-M. 1999. Electrostatic modulation of superconductivity in ultrathin $GdBa_2Cu_3O_{7-x}$ films. *Science* 284:1152–53
7. von Helmholtz HLF. 1853. Ueber einige Gesetze der Vertheilung elektrischer Ströme in körperlichen Leitern mit Anwendung auf die thierisch-elektrischen Versuche. *Ann. Phys.* 89:211–33
8. Hong X, Posadas A, Lin A, Ahn CH. 2003. Ferroelectric-field-induced tuning of magnetism in the colossal magnetoresistive oxide $La_{1-x}Sr_xMnO_3$. *Phys. Rev. B* 68:134415
9. Vaz CAF, Hoffman J, Segal Y, Reiner JW, Grober RD, et al. 2010. Origin of the magnetoelectric coupling effect in $Pb(Zr_{0.2}Ti_{0.8})O_3/La_{0.8}Sr_{0.2}MnO_3$ multiferroic heterostructures. *Phys. Rev. Lett.* 104:127202
10. Hajo J, Molegraaf A, Hoffman J, Vaz CAF, Gariglio S, et al. 2009. Magnetoelectric effects in complex oxides with competing ground states. *Adv. Mater.* 21:3470–74
11. Hong X, Posadas A, Ahn CH. 2005. Examining the screening limit of field effect devices via the metal-insulator transition. *Appl. Phys. Lett.* 86:142501
12. Ramesh R, Spaldin NA. 2007. Multiferroics: progress and prospects in thin films. *Nat. Mater.* 6:21–29
13. Bozovic I, Matijasevic J. 2000. COMBE: a powerful new tool for materials science. *Mater. Sci. Forum* 352:1–8
14. Xi XX, Doughty C, Walkenhorst A, Kwon C, Li Q, Venkatesan T. 1992. Effects of field-induced hole-density modulation on normal-state and superconducting transport in $YBa_2Cu_3O_{7-x}$. *Phys. Rev. Lett.* 68:1240–43
15. Nakamura T, Tokuda H, Tanaka S, Iiyama M. 1996. Dielectric properties of $SrTiO_3$ thin films grown by ozone-assisted molecular beam epitaxy. *Jpn. J. Appl. Phys.* 34:1906–10
16. Muller KA, Birkard J. 1979. $SrTiO_3$: an intrinsic quantum paraelectric below 4 K. *Phys. Rev. B* 19:3593–602
17. Matthey D, Gariglio S, Triscone J-M. 2003. Field-effect experiments in $NdBa_2Cu_3O_{7-\delta}$ ultrathin films using a $SrTiO_3$ single-crystal gate insulator. *Appl. Phys. Lett.* 83:2758–3760
18. Koster G, Kropman BL, Rijnders GJHM, Blank DHA, Rogalla H. 1998. Quasi-ideal strontium titanate crystal surfaces through formation of strontium hydroxide. *Appl. Phys. Lett.* 73:2920–22
19. Bhattacharya A, Eblen-Zayas M, Staley N, Huber WH, Goldman AM. 2004. Micromachined $SrTiO_3$ single crystals as dielectrics for electrostatic doping of thin films. *Appl. Phys. Lett.* 85:997–99
20. Robertson J. 2004. High dielectric constant oxides. *Eur. Phys. J. Appl. Phys.* 28:265–91
21. Leng X, Garcia-Barriocanal J, Bose S, Lee Y, Goldman AM. 2011. Electrostatic control of the evolution from a superconducting phase to an insulating phase in ultrathin $YBa_2Cu_3O_{7-x}$ films. *Phys. Rev. Lett.* 107:027001
22. Sato T, Masuda G, Takagi K. 2004. Electrochemical properties of novel ionic liquids for electric double layer capacitor applications. *Electrochem. Acta* 49:3603–11

23. Zhang S, Sun N, He X, Lu X, Zhang X. 2006. Physical properties of ionic liquids: database and evaluation. *J. Phys. Chem. Ref. Data* 35:1475–503
24. Fujimoto T, Awaga K. 2013. Electric-double-layer field-effect transistors with ionic liquids. *Phys. Chem. Chem. Phys.* 15:8983–9006
25. Panzer MJ, Newman CR, Frisbie CD. 2005. Low-voltage operation of a pentacene field-effect transistor with a polymer electrolyte gate dielectric. *Appl. Phys. Lett.* 86:103503
26. Panzer MJ, Frisbie CD. 2005. Polymer electrolyte gate dielectric reveals finite windows of high conductivity in organic thin film transistors at high charge carrier densities. *J. Am. Chem. Soc.* 127:6960–61
27. Panzer MJ, Frisbie CD. 2006. High charge carrier densities and conductance maxima in single-crystal organic field-effect transistors with a polymer electrolyte gate dielectric. *Appl. Phys. Lett.* 88:203504
28. Dhoot AS, Yuen JD, Heeney M, McCulloch I, Moses D, Heeger AJ. 2006. Beyond the metal-insulator transition in polymer electrolyte gated polymer field-effect transistors. *Proc. Natl. Acad. Sci. USA* 103:11834–37
29. Lee J, Kaake LG, Cho JH, Zhu XY, Lodge TP, Frisbie CD. 2009. Ion gel-gated thin-film transistors: operating mechanism and characterization of gate dielectric capacitance, switching speed, and stability. *J. Phys. Chem. C* 113:8972–81
30. Brattain WH, Garrett CGB. 1955. Experiments on the interface between germanium and an electrolyte. *Bell Syst. Tech. J.* 34:129–76
31. Haupt SG, Riley DR, Zhau J, Zhou JP, Grassi JH, McDevitt JT. 1994. Reversible modulation of superconductivity in $YBa_2Cu_3O_{7-\delta}$/polypyrrole sandwich structures. *SPIE Symp. Ser. Supercond. Devices* 1258:238–49
32. Ye JT, Inoue S, Kobayashi K, Kasahara Y, Yuan HT, et al. 2010. Liquid-gated interface superconductivity on an atomically flat film. *Nat. Mater.* 9:125–28
33. Kasahara Y, Nishijima T, Sato T, Takeuchi Y, Ye J, et al. 2011. Electric-field-induced superconductivity detected by magnetization measurements of an electric-double-layer capacitor. *J. Phys. Soc. Jpn.* 80:023708
34. Ueno K, Nakamura S, Shimmotani H, Ohtomo A, Kimura N, et al. 2008. Electric-field-induced superconductivity in an insulator. *Nat. Mater.* 7:855–58
35. Lee Y, Clement C, Hellerstedt J, Kinney J, Kinnischtzke L, et al. 2011. Phase diagram of electrostatically doped $SrTiO_3$. *Phys. Rev. Lett.* 106:136809
36. Ueno K, Nakamura S, Shimotani H, Yuan HT, Kimura N, et al. 2011. Discovery of superconductivity in $KTaO_3$ by electrostatic carrier doping. *Nat. Nanotechnol.* 6:408–12
37. Taniguchi K, Matsumoto A, Shimotani H, Takagi H. 2012. Electric-field-induced superconductivity at 9.4 K in a layered transition metal disulphide MoS_2. *Appl. Phys. Lett.* 101:042603
38. Ye JT, Zhang YJ, Akashi R, Bahramy MS, Arita R, Iwasa Y. 2012. Superconducting dome in a gate-tuned band insulator. *Science* 338:1193–96
39. Bollinger AT, Dubuis G, Yoon J, Pavuna D, Misewich J, Bozovic I. 2011. Superconductor-insulator transition in $La_{2-x}Sr_xCuO_4$ at the pair quantum resistance. *Nature* 472:458–60
40. Dubuis G, Bollinger AT, Pavuna D, Bozovic I. 2012. Electric field effect on superconductivity in $La_{2-x}Sr_xCuO_4$. *J. Appl. Phys.* 111:112632
41. Leng X, Garcia-Barriocanal J, Yang B, Lee Y, Kinney J, Goldman AM. 2012. Indications of an electronic phase transition in two-dimensional superconducting $YBa_2Cu_3O_{7-x}$ thin films induced by electrostatic doping. *Phys. Rev. Lett.* 108:067004
42. Garcia-Barriocanal J, Kobrinskii A, Leng X, Kinney J, Yang B, et al. 2013. Electronically driven superconductor-insulator transition in electrostatically doped $La_2CuO_{4+\delta}$ films. *Phys. Rev. B* 87:024509
43. Lee Y, Frydman A, Chen T, Skinner B, Goldman AM. 2013. Electrostatic tuning of the properties of disordered indium-oxide films near the superconductor-insulator transition. *Phys. Rev. B* 88:024509
44. Dhoot AS, Israel C, Moya X, Mathur ND, Friend RH. 2009. Large electric field effect in electrolyte-gated manganites. *Phys. Rev. Lett.* 102:136502
45. Yuan H, Shimotani H, Tsukazaki A, Ohtomo A, Kawasaki M, Iwasa Y. 2009. High-density carrier accumulation in ZnO field-effect transistors gated by electric double layers of ionic liquids. *Adv. Funct. Mater.* 19:1046–53

46. Asanuma S, Xiang P-H, Yamada H, Sato H, Inoue IH, et al. 2010. Tuning of the metal-insulator transition in electrolyte-gated $NdNiO_3$. *Appl. Phys. Lett.* 97:142110
47. Hormoz S, Ramanathan S. 2010. Limits on vanadium oxide Mott metal-insulator transition field-effect transistors. *Solid State Electron.* 54:654–59
48. Ruzmetov D, Gopalakrishnan G, Ko C, Narayanamurti V, Ramanathan S. 2010. Three-terminal field effect devices utilizing thin film vanadium oxide as the channel layer. *J. Appl. Phys.* 107:114516
49. Zhang Y, Ye J, Matsuhashi Y, Iwasa Y. 2012. Ambipolar MoS_2 thin flake transistors. *Nano Lett.* 12:1136–40
50. Zhou Y, Ramanathan S. 2012. Relaxation dynamics of ionic liquid–VO_2 interfaces and influence of electric double-layer transistors. *J. Appl. Phys.* 111:084508
51. Yang Z, Zhou Y, Ramanathan S. 2012. Studies on room-temperature electric-field effect in ionic-liquid gated VO_2 three-terminal devices. *J. Appl. Phys.* 111:014506
52. Nakano M, Shibuya K, Okuyama D, Hatano T, Ono S, et al. 2012. Collective bulk carrier delocalization driven by electrostatic surface charge accumulation. *Nature* 487:459–62
53. Jeong J, Aetukuri N, Graf T, Schladt TD, Smant MG, Parkin SSP. 2013. Suppression of metal-insulator transition in VO_2 by electric field–induced oxygen vacancy formation. *Science* 339:1402–5
54. Xia Y, Xie W, Ruden PP, Frisbie CD. 2010. Carrier localization on surfaces of organic semiconductors gated with electrolytes. *Phys. Rev. Lett.* 105:036802
55. Sato T, Masuda G, Takagi K. 2004. Electrochemical properties of novel ionic liquids for electric double layer capacitor applications. *Electrochem. Acta* 49:3603–11
56. Bier M, Dietrich S. 2010. Vapour pressure of ionic liquids. *Mol. Phys.* 108:211–14
57. Oldham KB. 2008. A Gouy–Chapman–Stern model of the double layer at a (metal)/(ionic liquid) interface. *J. Electroanal. Chem.* 612:131–38
58. Glover RE III, Sherrill MD. 1960. Changes in superconducting critical temperature produced by electrostatic charging. *Phys. Rev. Lett.* 5:248–50
59. Stadler HL. 1965. Changing properties of metals by ferroelectric polarization charging. *Phys. Rev. Lett.* 14:979–81
60. Fiory AT, Hebard AF. 1985. Field-effect and electron density modulation of the superconducting transition in composite In/InO_x thin films. *Physica B* 135:124–27
61. Misra R, McCarthy M, Hebard AF. 2007. Electric field gating with ionic liquids. *Appl. Phys. Lett.* 90:052905
62. Lee Y, Frydman A, Chen T, Skinner B, Goldman AM. 2013. Electrostatic tuning of the properties of disordered indium-oxide films near the superconductor-insulator transition. *Phys. Rev. B* 88:024509
63. Parendo KA, Tan KHSB, Bhattacharya A, Eblen-Zayas M, Staley NE, Goldman AM. 2005. Electrostatic tuning of the superconductor-insulator transition in two dimensions. *Phys. Rev. Lett.* 94:197004
64. Millis AJ. 2003. Towards a classification of the effects of disorder on materials properties. *Solid State Commun.* 126:3–8
65. Matijasevic VC, Boogers S, Chen NY, Appleboom HM, Hadley P, Mooij JE. 1994. Electric field induced superconductivity in an overdoped cuprate superconductor. *Physica C* 235–240:2097–98
66. Cassinese A, De Luca GM, Prigiobbo A, Salluzzo M, Vaglio R. 2004. Field-effect tuning of carrier density in $Nd_{1.2}Ba_{1.8}Cu_3O_y$ thin films. *Appl. Phys. Lett.* 84:3933–35
67. Rufenacht A, Locquet JP, Fompeyrine J, Caimi D, Martinoli P. 2006. Electrostatic modulation of the superfluid density in an ultrathin $La_{2-x}Sr_xCuO_4$ film. *Phys. Rev. Lett.* 96:227002
68. Matthey D, Reyren N, Triscone J-M. 2007. Electric-field-effect modulation of the transition temperature mobile carrier density and in-plane penetration depth of $NdBa_2Cu_3O_{7-\delta}$ thin films. *Phys. Rev. Lett.* 98:057002
69. Salluzzo M, Ghiringhelli G, Cezar JC, Brookes NB, De Luca GM, et al. 2008. Indirect electric field doping of the CuO_2 planes of the cuprate $NdBa_2Cu_3O_7$ superconductor. *Phys. Rev. Lett.* 100:056810
70. Brookes NB, Ghiringhelli G, Cezar JC, De Luca GM, Salluzzo M. 2009. An X-ray absorption study of the electric field effect mechanism in "123" cuprates. *Eur. Phys. J. B* 70:153–56
71. Dhoot AS, Wimbush SC, Benseman T, MacManus-Driscol JL, Cooper JR, Friend RH. 2010. Increased T_c in electrolyte-gated cuprates. *Adv. Mater.* 22:2529–33

72. Chandrasekhar N, Valls OT, Goldman AM. 1993. Mechanism for electric-field effects observed in $YBa_2Cu_3O_{7-x}$ films. *Phys. Rev. Lett.* 71:1079–82
73. Sondhi SL, Girvin SM, Carini JP, Shahar D. 1997. Continuous quantum phase transitions. *Rev. Mod. Phys.* 69:315–33
74. Nojima R, Tada H, Nakamura S, Kobayashi N, Shimotani H, Iwasa Y. 2011. Hole reduction and electron accumulation in $YBa_2Cu_3O_y$ thin films using an electrochemical technique: evidence for an *n*-type metallic state. *Phys. Rev. B* 84:020502(R)
75. Leng X, Garcia-Barriocanal J, Kinney J, Yang B, Lee Y, Goldman AM. 2013. Electrostatic tuning of the superconductor to insulator transition of $YBa_2Cu_3O_{7-x}$ using ionic liquids. *J. Phys. Conf. Ser.* 449:012009
76. Salamon MB, Jaime M. 2001. The physics of manganites: structure and transport. *Rev. Mod. Phys.* 73:583–628
77. Ogale SB, Talyansky V, Chen CH, Ramesh R, Greene RL, Benkatesan T. 1996. Unusual electric field effects in $Nd_{0.7}Sr_{0.3}MnO_3$. *Phys. Rev. Lett.* 77:1159–62
78. Hong X, Posadas A, Lin A, Ahn CH. 2003. Ferroelectric-field-induced tuning of magnetism in the colossal magnetoresistive oxide $La_{1-x}Sr_xMnO_3$. *Phys. Rev. B* 68:134415
79. Eblen-Zayas M, Bhattacharya A, Staley NE, Kobrinskii AL, Goldman AM. 2005. Ambipolar gate effect and low temperature magnetoresistance of ultrathin $La_{0.8}Ca_{0.2}MnO_3$ films. *Phys. Rev. Lett.* 94:037204
80. Chiba D, Yamanouchi M, Matsukura F, Ohno H. 2003. Electrical manipulation of magnetization reversal in a ferromagnetic semiconductor. *Science* 301:943–45
81. Nakayama H, Ye J, Ohtani T, Fujikawa Y, Ando K, et al. 2012. Electroresistance effect in gold thin film induced by ionic-liquid-gated electric double layer. *Appl. Phys. Express* 5:023002
82. Scherwitzl R, Zubko P, Lichtensteiger C, Triscone J-M. 2009. Electric-field tuning of the metal-insulator transition in ultrathin films of $LaNiO_3$. *Appl. Phys. Lett.* 95:222114
83. Scherwitzl R, Zubko P, Lezama G, Ono S, Morpurgo AF, et al. 2010. Electric-field control of the metal-insulator transition in ultrathin $NdNiO_3$ films. *Adv. Mater.* 22:5527–20
84. Asanuma S, Xiang P-H, Yamada H, Sato H, Inoue IH, et al. 2010. Tuning of the metal-insulator transition in electrolyte-gated $NdNiO_3$. *Appl. Phys. Lett.* 97:142110
85. Kim H-T, Lee YW, Kim BJ, Chae BG, Yun SJ, et al. 2006. Monoclinic and correlated metal phase in VO_2 as evidence of the Mott transition: correlated photon analysis. *Phys. Rev. Lett.* 97:266401
86. Chen C, Wang R, Lang S, Guo C. 2008. Gate-field-induced phase transitions in VO_2: monoclinic metal phase separation and switchable infrared reflections. *Appl. Phys. Lett.* 93:171101
87. Hormoz S, Ramanathan S. 2010. Limits on vanadium oxide Mott metal-insulator transition field-effect transistors. *Solid State Electron.* 54:654–59
88. Ruzmetov D, Gopalakrishnan G, Ko C, Narayanamurti V, Ramanathan S. 2010. Three-terminal field effect devices utilizing thin film vanadium oxide as the channel layer. *J. Appl. Phys.* 107:114516
89. Ji H, Wei J, Natelson D. 2012. Modulation of the electrical properties of VO_2 nanobeams using an ionic liquid as a gating medium. *Nano Lett.* 12:2988–92
90. Yang Z, Zhou Y, Ramanathan S. 2012. Studies on room-temperature electric-field effect in ionic-liquid gated VO_2 three-terminal devices. *J. Appl. Phys.* 111:014506